



Article

# Genome-Wide Identification, Evolution, and Expression Analysis of the WD40 Subfamily in *Oryza* Genus

Simin Ke , Yifei Jiang, Mingao Zhou and Yangsheng Li \*

State Key Laboratory of Hybrid Rice, College of Life Sciences, Wuhan University, Wuhan 430072, China; 2021202040080@whu.edu.cn (S.K.); 2021102040039@whu.edu.cn (Y.J.); 2021202040077@whu.edu.cn (M.Z.)

\* Correspondence: lysh2001@whu.edu.cn

**Abstract:** The WD40 superfamily is widely found in eukaryotes and has essential subunits that serve as scaffolds for protein complexes. WD40 proteins play important regulatory roles in plant development and physiological processes, such as transcription regulation and signal transduction; it is also involved in anthocyanin biosynthesis. In rice, only *OsTTG1* was found to be associated with anthocyanin biosynthesis, and evolutionary analysis of the WD40 gene family in multiple species is less studied. Here, a genome-wide analysis of the subfamily belonging to WD40-TTG1 was performed in nine AA genome species: *Oryza sativa* ssp. *japonica*, *Oryza sativa* ssp. *indica*, *Oryza rufipogon*, *Oryza glaberrima*, *Oryza meridionalis*, *Oryza barthii*, *Oryza glumaepatula*, *Oryza nivara*, and *Oryza longistaminata*. In this study, 383 WD40 genes in the *Oryza* genus were identified, and they were classified into four groups by phylogenetic analysis, with most members in group C and group D. They were found to be unevenly distributed across 12 chromosomes. A total of 39 collinear gene pairs were identified in the *Oryza* genus, and all were segmental duplications. WD40s had similar expansion patterns in the *Oryza* genus. Ka/Ks analyses indicated that they had undergone mainly purifying selection during evolution. Furthermore, WD40s in the *Oryza* genus have similar evolutionary patterns, so *Oryza sativa* ssp. *indica* was used as a model species for further analysis. The cis-acting elements analysis showed that many genes were related to jasmonic acid and light response. Among them, *OsiWD40-26/37/42* contained elements of flavonoid synthesis, and *OsiWD40-15* had MYB binding sites, indicating that they might be related to anthocyanin synthesis. The expression profile analysis at different stages revealed that most *OsiWD40s* were expressed in leaves, roots, and panicles. The expression of *OsiWD40s* was further analyzed by qRT-PCR in 9311 (*indica*) under various hormone treatments and abiotic stresses. *OsiWD40-24* was found to be responsive to both phytohormones and abiotic stresses, suggesting that it might play an important role in plant stress resistance. And many *OsiWD40s* might be more involved in cold stress tolerance. These findings contribute to a better understanding of the evolution of the WD40 subfamily. The analyzed candidate genes can be used for the exploration of practical applications in rice, such as cultivar culture for colored rice, stress tolerance varieties, and morphological marker development.



**Citation:** Ke, S.; Jiang, Y.; Zhou, M.; Li, Y. Genome-Wide Identification, Evolution, and Expression Analysis of the WD40 Subfamily in *Oryza* Genus. *Int. J. Mol. Sci.* **2023**, *24*, 15776. <https://doi.org/10.3390/ijms242115776>

Academic Editors: Alexandra S. Dubrovina and Konstantin V. Kiselev

Received: 12 September 2023

Revised: 23 October 2023

Accepted: 27 October 2023

Published: 30 October 2023

**Keywords:** rice; *Oryza* genus; WD 40; expression patterns; gene family



**Copyright:** © 2023 by the authors. Licensee MDPI, Basel, Switzerland. This article is an open access article distributed under the terms and conditions of the Creative Commons Attribution (CC BY) license (<https://creativecommons.org/licenses/by/4.0/>).

## 1. Introduction

WD40, also known as the WD-repeat (WDR) protein, is a family of proteins that have been highly conserved during evolution, and they are widely found in eukaryotes [1]. The WD40 domain is generally 4–8 amino acid residues of about 40–60, containing a glycine–histidine dimer peptide (GH) at the N-terminal end and a tryptophan–aspartate dimeric peptide (WD) at the C-terminal end [2,3]. Typically, the WD40 domain has a  $\beta$ -propeller structure containing 4–9 blades, and its scaffold-type structure can serve as an interaction site for a variety of biomolecules, including proteins, peptides, RNA, and DNA, which helps proteins exert their biological activities [4–6]. WD40 proteins have complex structures and functions; they can interact with diverse proteins in various ways and are involved in

many bioregulatory processes such as DNA replication, damage response, transcriptional regulation, post-translational modification, signal transduction, and apoptosis [7–10]. In addition, most WD40 proteins are found in eukaryotes, and only a small fraction is found in prokaryotes [11]. In lower organisms, WD40 is mainly involved in cell cycle, growth, and development, while in higher organisms, it plays an important role in cell cycle, apoptosis, signal transduction, abiotic stress, and other physiological and biochemical processes [12–14].

Previously, the researchers classified WD40 proteins in different species based on evolutionary relationships and sequence similarity. Due to low sequence conservation and high functional diversity of the WD40 family, 237 potential *AtWD40* proteins containing at least 4 WDR motifs were identified in *Arabidopsis thaliana* and classified into 33 groups [15]; in the peach genome, 220 WD40 superfamily members were identified, and the *MtWD40s* were further divided into five subfamilies based on grouping in *Arabidopsis thaliana* [16]; physiological biochemistry, genetic structure and conserved protein motifs of 42 *JrWD40s* were identified and analyzed in walnut [17]; in japonica rice, a total of 200 members of WD40 were identified and categorized into 11 subfamilies based on structural domain features [18]. A specialized database, WDSP “<http://wu.scbb.pkusz.edu.cn/wdsp/>” (accessed on 20 June 2023), has been developed to provide detailed information on WD40-repeat proteins of individual species. WDSPdb contains 63,211 WD40-repeat proteins identified in 3383 species, including most model organisms, and it can be used to view structural models, hotspot residues, etc. [19].

WD40 proteins generally have additional structural domains to recruit other factors to form protein–protein complexes [20]. Therefore, the WD40 protein family participates in many plant development and physiological processes and regulates the assembly of multiple complexes in plant resistance and abiotic stress response [21–23]. For example, in wheat (*Triticum aestivum* L.), *TaWD40D* encoding seven WD40 domains was identified, which was a positive regulator of plant responses to salt stress and osmotic stress. The down-regulation of it resulted in decreased relative water content and impaired growth [24]. In tomato (*Solanum lycopersicum*), *SIWD40* was strongly co-expressed with master regulators such as RIN (ripening inhibitor) and NOR (nonripening). And *SIWD40* overexpression and RNAi lines exhibited substantially accelerated and delayed phenotypes compared with the wild type, respectively [25]. In rice, *OsLIS-L1* containing WD40 motifs played an important role in male gametophyte formation and the first internode elongation [26].

The most widely known function of WD40 is as part of the MYB-bHLH-WD40 (MBW) complex, involved in the regulation of anthocyanin/proanthocyanin biosynthesis. Anthocyanins are antioxidants used as natural colorants and are beneficial to human health, which contributes to reactive oxygen species detoxification and sustains plant growth and development [27]. The first WD40 protein related to anthocyanins biosynthesis identified in the model plant *Arabidopsis* was TRANSPARENT TESTA GLABRA1 (TTG1). *AtTTG1* encodes 341 amino acids and can form an MBW ternary complex with *AtMYB123* and *AtbHLH42* to synergistically activate the expression of BANYULS (anthocyanidin reductase) expression and promote the biosynthesis of proanthocyanin [28]. In contrast, the codon of the *Atttg1* mutant is terminated early, the *AtTTG1* protein is truncated at the far C-terminus, and the seedlings are unable to accumulate anthocyanins [29]. *Oryza sativa* ssp. *japonica* *OsTTG1*, *Vitis vinifera* (grape) *VvWDR1*, and *Camellia sinensis* *CsWD40* encode 355, 344, and 342 amino acids, respectively. In the *Osttg1* mutant of the DLMM rice variety, there was almost no anthocyanin accumulation in the rice bast, and the pericarp was nearly white, with only the abaxial side brown [30]. Overexpression of TTG1-like *CsWD40* in tobacco resulted in a significant increase in anthocyanin content in petals of transgenic plants; both anthocyanin and proanthocyanin content were increased when co-expressed with *CsMYB5e* in tobacco [31]. *VvWDR1* increases anthocyanin accumulation in transgenic tobacco through interaction with the *VvMYBA2r-VvMYCA1* complex [32].

In addition to anthocyanin biosynthesis, studies have shown that TTG1 is also related to seed coat mucilage biosynthesis [33], root–hair pattern [34,35], flowering time regula-

tion [36], fruit spine initiation [37,38]. Among other processes, TTG1 might also directly or indirectly regulate downstream target genes through interactions with other proteins [39]. Current studies related to the regulation of TTG1 are more limited, and most of them dissociate the TTG1-containing MBW complex for regulation. For example, EIN3 and RSL4 interfere with WER-GL3-TTG1 (MBW complex) and mediate ectopic root hair formation in *Arabidopsis* [40], and SnRK1 inhibits anthocyanin biosynthesis through transcriptional regulation of the MYB-bHLH-TTG1 complex [41].

With the completion of the wild rice genome map, the *Oryza* genus is increasingly becoming an ideal system for evolutionary and functional genomics studies in gramineous plants. The AA genome is the genome type in the *Oryza* genus that contains the largest number and widest distribution of diploid species. The AA genome *Oryza* species is widely distributed in both natural and wild environments and contains many genes that can improve rice yield and stress tolerance [42,43]. However, there is no evolutionary analysis of the WD40 protein family in the *Oryza* genus. Therefore, the AA genome *Oryza* species was chosen to analyze the evolutionary relationships of the WD40 protein family. Since the WD40 protein family is enormous, this study will focus on the subfamily where *OsTTG1* is located and identify and analyze the WD40 subfamily in the rice AA genome, including *O. sativa japonica*, *O. sativa indica*, *O. longistaminata*, *O. barthii*, *O. glumaepatula*, *O. meridionalis*, *O. nivara*, *O. glaberrima* and *O. rufipogon*. Based on rigorous phylogenetic analysis, subfamily members were identified, and evolutionary relationships were inferred. In addition, 200 *OsWD40s* proteins were identified in japonica rice in previous studies [18], and the *Oryza* genus can be characterized similarly. Therefore, indica was chosen as a model plant for the analysis of cis-acting elements and expression patterns. The results provide a global view of the WD40-TTG1 subfamily in the AA genome *Oryza* genus, and candidate genes related to anthocyanins can be used to cultivate colored rice or develop morphological markers.

## 2. Results

### 2.1. Identification of WD40 Repeat Protein Family in *Oryza* Genus

In the reported study, a total of 200 members in japonica *OsWD40s* were identified, of which 50 members were in the subfamily where *OsTTG1* is located [18]. These 50 protein sequences were compared as queries in the remaining eight *Oryza* genera. After removing the duplicate sequences, a total of 383 members of the subfamily in which WD40-TTG1 is located were identified, including *O. japonica*, of which 51 in *O. sativa indica*, 9 in *O. longistaminata*, 48 in *O. barthii*, 46 in *O. glumaepatula*, 37 in *O. meridionalis*, 48 in *O. nivara*, 46 in *O. glaberrima*, 48 in *O. rufipogon*, 50 in *O. sativa japonica* (Figure 1a, Table S1). To understand their evolutionary relationships, we constructed a phylogenetic tree and divided it into four groups (Figure 1b). Among them, groups C and D had the most members, with 113 and 123 members, respectively. *OsTTG1* (*LOC\_Os02g45810*) was in group C, and indica *OsR498G0204537800.01* was close to it.

### 2.2. Characterization and Phylogenetic Relation of *OsiWD40* Family Members in *Indica*

To understand the overall distribution of WD40s on the genome, the gene distribution of family members was visualized. Additionally, the current genomic information of *Oryza longistaminata* is incomplete. Although the genome sequence has been sequenced, it has not been annotated and analyzed, so the chromosome distribution cannot be analyzed yet. Except for *Oryza longistaminata*, the distribution pattern of genes in the rest of the *Oryza* genus was similar (Figure 2a). They were widely and unevenly distributed on 12 chromosomes, and the highest numbers were found on their first five chromosomes, with fewer members in the remaining chromosomes. Next, chromosome distribution in indica was visualized, and its gene names were renamed in order (Figure 2b). The correlation coefficient between chromosome length and family gene numbers is 0.79, indicating that gene distribution showed a positive correlation with chromosome length.

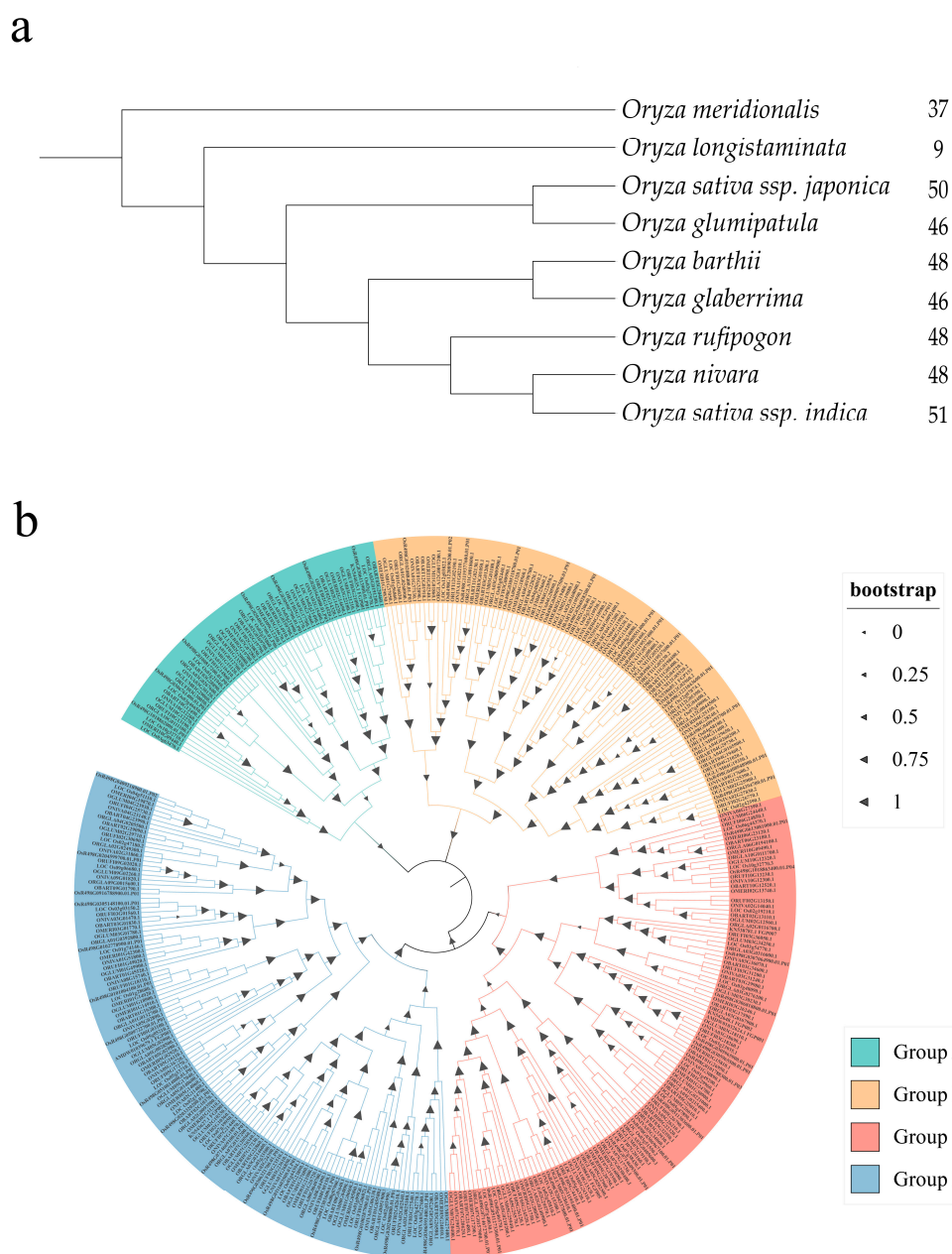


**Figure 1.** Phylogenetic relationship of WD40 repeat protein family identified in *Oryza* genus. (a) Tree based on divergence times and the number of members of the respective family is indicated next to the species name. (b) Phylogenetic tree of *Oryza* genus constructed based on the maximum likelihood method, divided into four groups: A, B, C, and D. The triangle size indicates the bootstrap value.

In addition, some physicochemical properties of WD40s were predicted (Table S2). WD40 gene members in *O. longistaminata* were fewer than other *Oryza* genera, but their amino acid numbers and molecular weight size range were wider than the rest of them, and the isoelectric point value changes were smaller. This might be due to its relatively homogeneous genetic background, and its proteins have diverse functions and structures that can adapt to different environmental pressures. Its isoelectric point range was small, indicating that most of its proteins carry negative charges, which might be related to its salt tolerance. Furthermore, the similarity of physicochemical properties of other *Oryza* genera suggested that they might have similar biochemical functions and structures. For example, in indica, the size of amino acids ranged from 72 (*Osi*WD40-49) to 888 (*Osi*WD40-36), and the predicted molecular weight ranged from 7861.78 (*Osi*WD40-49) to 97,991.2 (*Osi*WD40-36).

The theoretical isoelectric points ranged from 4.3 (*OsiWD40-26*) to 9.81 (*OsiWD40-49*), with 32 acid isoelectric points and 19 basic isoelectric points. Subcellular localization predictions showed that 292 WD40s proteins were localized in the nucleus, 67 in the chloroplast, 15 in the extracellular, and 8 in membrane systems and mitochondria. This finding implies that the subfamily might be primarily involved in intranuclear developmental processes.

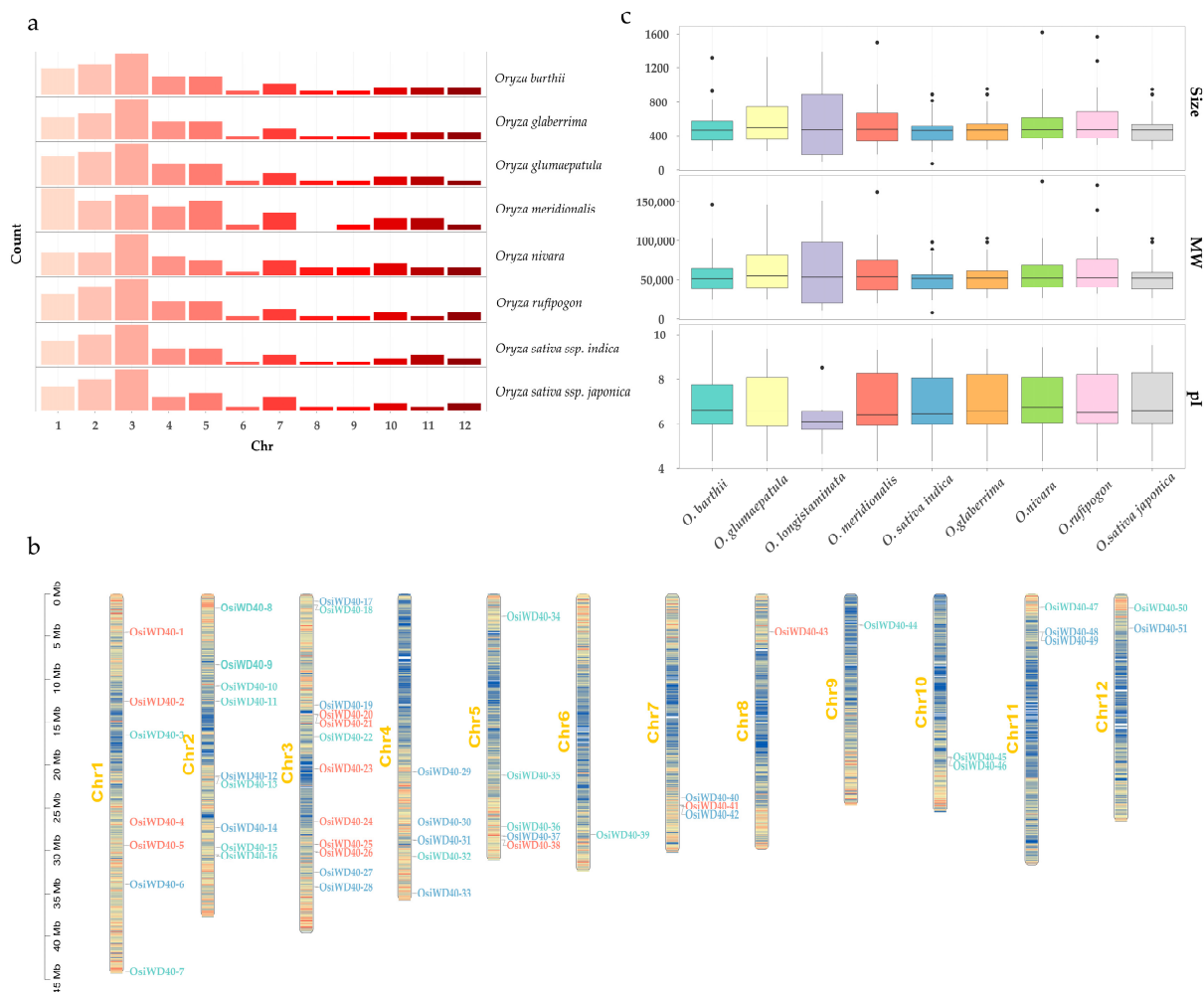


**Figure 2.** Chromosome distribution of the WD40s in *Oryza* genus. (a) The bar chart of the distribution of genes on chromosomes in each species. The x-axis is the chromosome number, and the y-axis is the gene count. The right side of the bar graph shows the corresponding species name. (b) The bars represent chromosomes. Chromosome numbers are shown on the left side of the chromosome. The *OsiWD40* is labeled on the right side of the chromosome. The scale bar on the left side indicates the length of the chromosome. (c) The box plots of amino acid size, molecular weight, and isoelectric point in *Oryza* genus. The x-axis represents species name, and y-axis represents the size of each of the three metrics. The size of box reflects the range of data, the line inside represents the median, and the dots outside the box mean outliers.

### 2.3. Analysis of Gene Structure and Conserved Motifs

The evolution of protein families is mainly manifested by the diversity of gene structures and changes in conserved motifs. To better understand the structure of WD40 proteins in the *Oryza* genus, ten conserved motifs were analyzed using MEME software (v5.5.4), and their domains were validated using the CDD database (Figure S1). The WD40 subfamily proteins in the *Oryza* genus were interspersed in the phylogenetic tree. Specifically, based on the similarity of protein sequences, most WD40 proteins in the *Oryza* genus had matching homologs and shared similar conserved motifs and structural domains. For ease of

observation, *OsiWD40s*, members of the WD40 family in *O. sativa indica*, were extracted for structural characterization (Figure 3). The phylogenetic tree was constructed based on their protein sequences (Figure 3a), which can be divided into three subgroups. The conserved motif analysis showed that all *OsiWD40s* contained at least five or more motifs (Figure 3b). After performing the Tomtom algorithm search, motifs 1–4 and 9 all had Trp-Asp (WD) repeats signatures (Table S4). Among them, most of the proteins in subgroups I and III had similar motif types and numbers, while subgroup II mostly contained 10 conserved motifs. This might indicate that the protein functions in subgroup II were more distinct from those in the other two groups. Structural domain analysis of these family members showed that each member has either a WD40 structural domain or a WD40 superfamily structural domain and other specific structural domains in different subgroups (Figure 3c). In addition, analysis of the gene structure of *OsiWD40s* showed that *OsiWD40s* had relatively more introns, with most members having more than five introns (Figure 3d). While genes of the same subgroup share similar exon/intron structures, group I had relatively longer introns, while group II and group III had relatively shorter introns. These findings contribute to the understanding of the structural diversity of the WD40 subfamily.

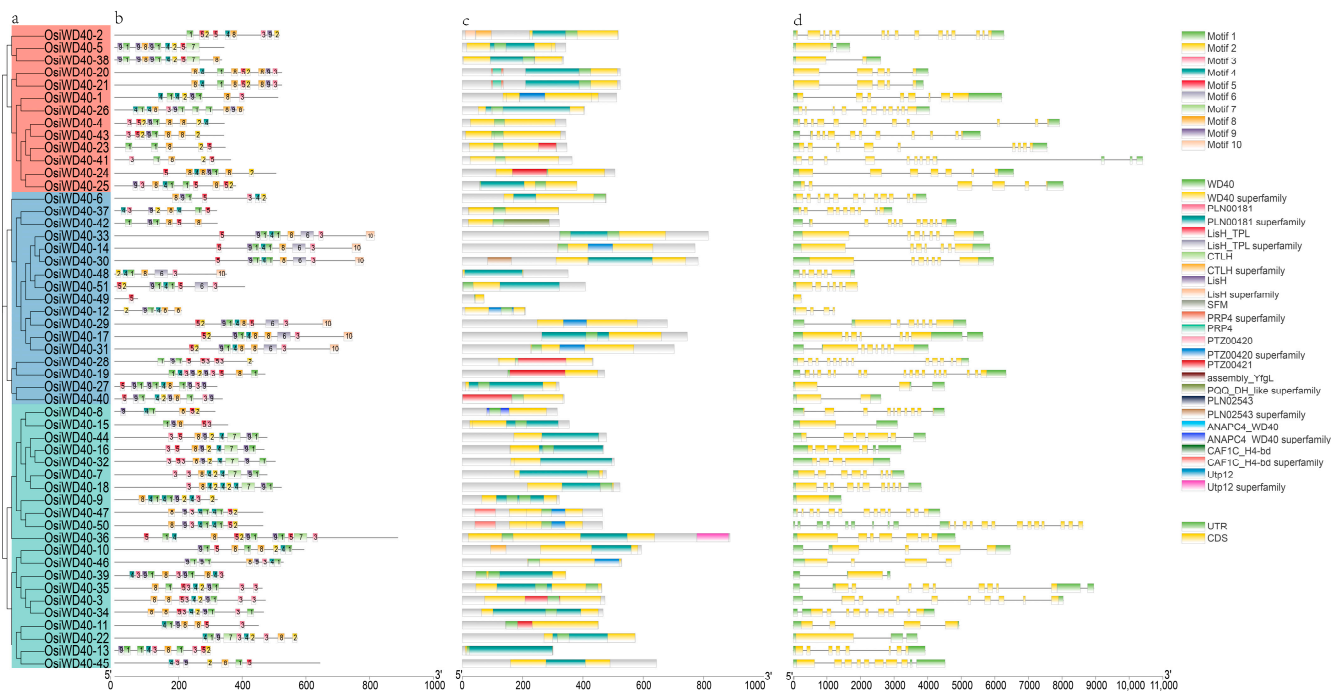


**Figure 3.** Phylogenetic relationship, conserved motifs, gene structure, and cis-acting factor of *OsiWD40s*. (a) An unrooted tree of *OsiWD40s* using fasttree based on protein sequences. The *OsiWD40s* was renamed. (b) Conserved motifs of *OsiWD40s* analyzed with MEME. (c) Domain prediction using CDD database. (d) Introns and exons of the *OsiWD40s*. Note: Different colors indicate different meanings; see the figure legends for details.

2.4. Collinearity Analysis of *OsiWD40s* in *Oryza* Genus

Gene duplication events are a critical part of gene family composition. Analysis of family gene duplication events with the Multiple Covariance Scanning (MCScanX) tool showed that, except *O. longistaminata*, in the remaining eight species *O. barthi*, *O. glaberrima*, *O. glumaepatula*, *O. sativa indica*, *O. meridionalis*, *O. nivara*, *O. rufipogon*, and *O. sativa japonica* a total of 6, 6, 5, 5, 3, 3, 5, and 6 collinear gene pairs were found (Table 1). The results showed that the duplication type of all collinear gene pairs was segmental/WGD duplication, and the gene pairs all showed a similar distribution in the genome, indicating that the expansion pattern of the WD40s was similar in multiple *Oryza* genera (Figure 4).

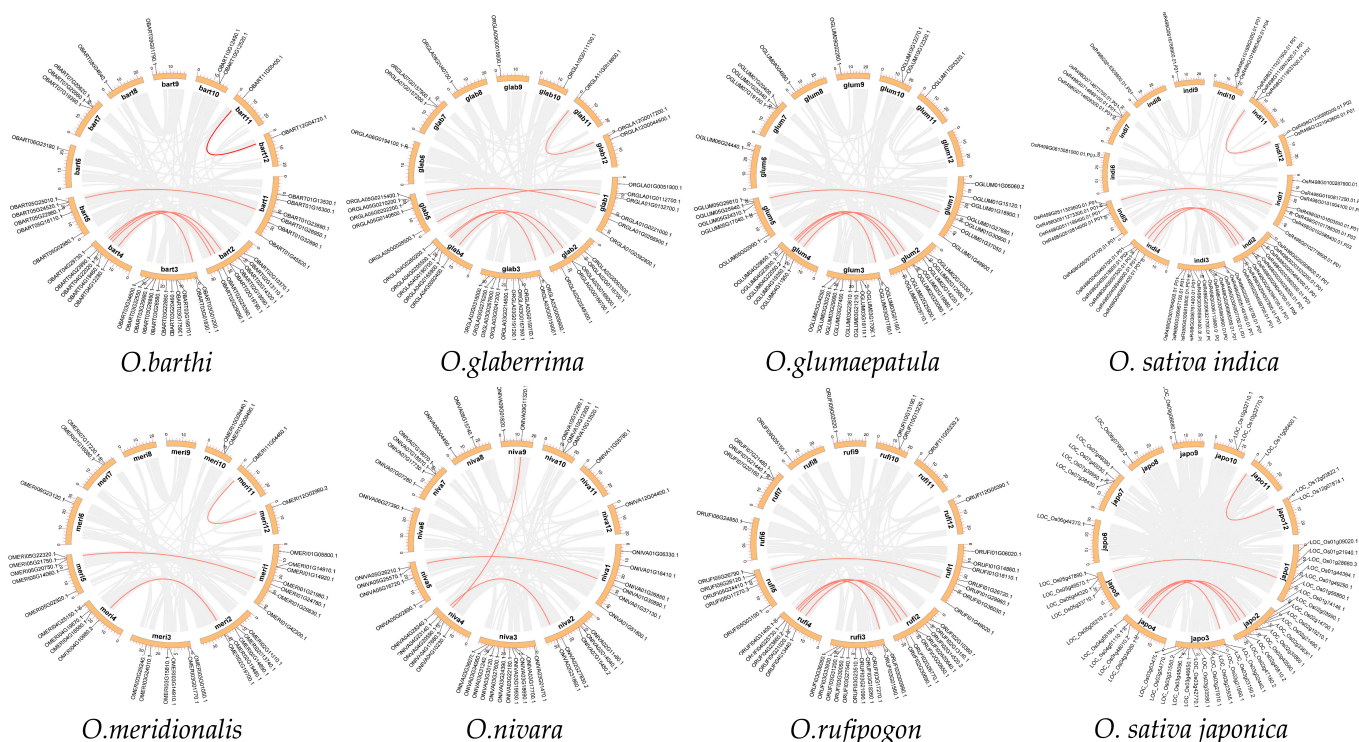


**Figure 4.** Collinearity analysis of *OsiWD40s* in *Oryza*. Collinear gene pairs are shown for eight species except for *O. longistaminata*. Red lines represent collinear gene pairs, and labels outside the circles are family member numbers for each species.

**Table 1.** The Ka/Ks values in duplicated gene pairs in *Oryza* genus.

<i>Oryza</i> Species	Gene Pairs	Ka/Ks	Date (Mya)	Type of Selection	Type of Duplication
<i>O. barthii</i>	<i>ObWD40-5/ObWD40-36</i>	0.24	40.76	Purifying	SD/WGD
	<i>ObWD40-46/ObWD40-48</i>	0.38	45.95	Purifying	SD/WGD
	<i>ObWD40-13/ObWD40-28</i>	0.28	68.50	Purifying	SD/WGD
	<i>ObWD40-15/ObWD40-30</i>	0.09	50.86	Purifying	SD/WGD
	<i>ObWD40-11/ObWD40-27</i>	0.22	133.43	Purifying	SD/WGD
	<i>ObWD40-16/ObWD40-29</i>	0.23	146.98	Purifying	SD/WGD
<i>O. glaberrima</i>	<i>OglaWD40-4/OglaWD40-34</i>	0.24	34.28	Purifying	SD/WGD
	<i>OglaWD40-3/OglaWD40-30</i>	0.17	90.11	Purifying	SD/WGD
	<i>OglaWD40-43/OglaWD40-45</i>	0.07	5.86	Purifying	SD/WGD
	<i>OglaWD40-10/OglaWD40-25</i>	0.22	129.39	Purifying	SD/WGD
	<i>OglaWD40-13/OglaWD40-28</i>	0.09	50.86	Purifying	SD/WGD
	<i>OglaWD40-14/OglaWD40-27</i>	0.23	146.07	Purifying	SD/WGD
<i>O. glumaepatula</i>	<i>OgluWD40-5/OgluWD40-35</i>	0.23	37.97	Purifying	SD/WGD
	<i>OgluWD40-11/OgluWD40-26</i>	0.21	131.89	Purifying	SD/WGD
	<i>OgluWD40-13/OgluWD40-27</i>	0.23	59.40	Purifying	SD/WGD
	<i>OgluWD40-15/OgluWD40-29</i>	0.14	56.44	Purifying	SD/WGD
	<i>OgluWD40-16/OgluWD40-28</i>	0.23	145.73	Purifying	SD/WGD
<i>O. indica</i>	<i>OsiWD40-5/OsiWD40-38</i>	0.27	33.55	Purifying	SD/WGD
	<i>OsiWD40-12/OsiWD40-29</i>	0.12	125.12	Purifying	SD/WGD
	<i>OsiWD40-14/OsiWD40-30</i>	0.23	60.94	Purifying	SD/WGD
	<i>OsiWD40-16/OsiWD40-32</i>	0.09	49.85	Purifying	SD/WGD
	<i>OsiWD40-47/OsiWD40-50</i>	0.08	5.03	Purifying	SD/WGD

Table 1. Cont.

<i>Oryza</i> Species	Gene Pairs	Ka/Ks	Date (Mya)	Type of Selection	Type of Duplication
<i>O. meridionalis</i>	<i>OmWD40-5/OmWD40-27</i>	0.23	58.16	Purifying	SD/WGD
	<i>OmWD40-36/OmWD40-37</i>	0.53	56.54	Purifying	SD/WGD
	<i>OmWD40-11/OmWD40-19</i>	0.25	126.22	Purifying	SD/WGD
<i>O. nivara</i>	<i>OnWD40-4/OnWD40-32</i>	0.22	144.04	Purifying	SD/WGD
	<i>OnWD40-12/OnWD40-27</i>	0.10	34.58	Purifying	SD/WGD
	<i>OnWD40-26/OnWD40-41</i>	0.25	41.55	Purifying	SD/WGD
<i>O. rufipogon</i>	<i>OrWD40-5/OrWD40-37</i>	0.23	52.06	Purifying	SD/WGD
	<i>OrWD40-14/OrWD40-29</i>	0.23	43.46	Purifying	SD/WGD
	<i>OrWD40-16/OrWD40-31</i>	0.14	129.31	Purifying	SD/WGD
	<i>OrWD40-12/OrWD40-28</i>	0.23	115.74	Purifying	SD/WGD
	<i>OrWD40-17/OrWD40-30</i>	0.23	123.19	Purifying	SD/WGD
<i>O. japonica</i>	<i>OsWD40-5/OsWD40-37</i>	0.23	34.98	Purifying	SD/WGD
	<i>OsWD40-47/OsWD40-48</i>	0.08	4.48	Purifying	SD/WGD
	<i>OsWD40-14/OsWD40-30</i>	0.26	64.56	Purifying	SD/WGD
	<i>OsWD40-16/OsWD40-31</i>	0.10	49.85	Purifying	SD/WGD
	<i>OsWD40-12/OsWD40-29</i>	0.22	129.57	Purifying	SD/WGD
	<i>OsWD40-17/OsWD40-30</i>	0.21	155.10	Purifying	SD/WGD

The Ka/Ks values of collinear gene pairs were used to assess the selection pressure of gene duplication. In general, Ka/Ks <1, =1, and >1 indicate that the genes are under purifying, neutral, and positive selection accordingly. The Ka/Ks values of all covariate gene pairs in the *Oryza* genus were less than 1, indicating that these genes had undergone strong purifying selection during evolution. In addition, the occurrence of replication events was calculated to range from 4.48 to 155.10 Mya for the gene pairs of eight *Oryza* genera.

#### 2.5. Analysis of Cis-Regulatory Elements (CREs) in the Promoters of *OsiWD40s*

In recent years, with the advancement of high-throughput sequencing technology and the completion of sequencing of various plant genomes, the analysis of promoter sequences and cis-elements has played a role in predicting the function of regulatory genes. In order to understand the genetic function, metabolic network, and regulatory mechanism of WD40, the cis-acting elements of the promoter region can be analyzed. And, from the previous analysis, the physiological characteristics and structure of the *Oryza* genus were similar; indica was used as a model plant to analyze its cis-acting elements. The 2000 bp upstream sequence of *OsiWD40s* was taken as the hypothetical promoter, and its distribution and function were analyzed and visualized (Figure 5a). A total of 46 elements were identified after collating the structures, which can be divided into four major categories: abiotic, elements related to drought and low-temperature responses; hormone-related, elements related to plant hormones such as MeJA and abscisic acid; development-related, elements specifically expressed in various organ tissues; and light responsive elements (Figure 5c–e). *OsiWD40s* had a larger variety of elements associated with light responsive, while the variety of elements associated with hormone-related and abiotic was small but numerous (Figure 5b). Almost all members contained hormone-related cis-regulatory elements, suggesting that the expression of *OsiWD40s* genes might be responsive to various plant hormones. Furthermore, the cis-element of *OsiWD40-26*, 37, and 42 were shown to be associated with flavonoid biosynthetic gene regulation. And *OsiWD40-15* had MYB binding sites and 11 hormone-related elements, including MeJA and gibberellin. The protein interaction analysis of *OsiWD40-15* also revealed that it interacted with four bHLH proteins, as well as two proteins containing HTH myb-type structural domains (Figure S2), showing that it might be involved in anthocyanin regulatory pathways as a member of the MBW complex.

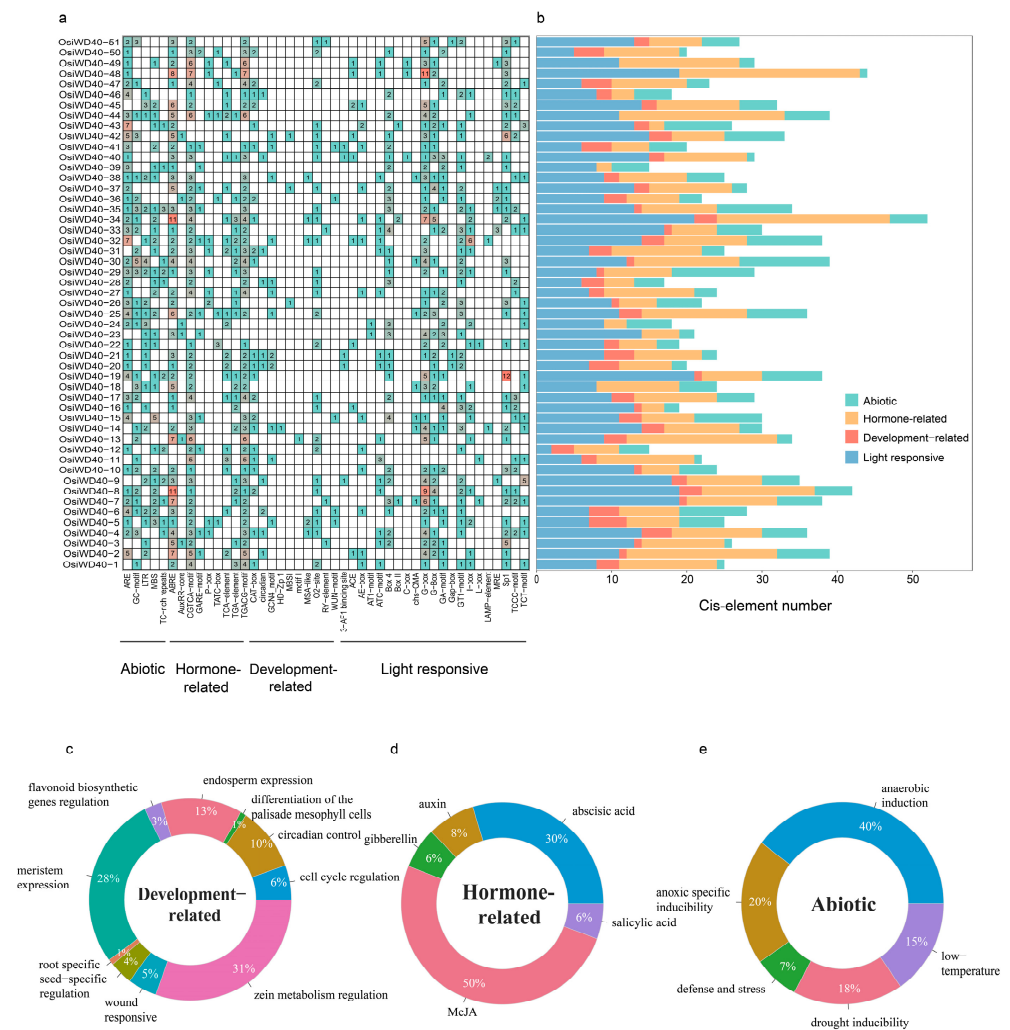


**Figure 5.** Predicted cis-elements of the *OsiWD40* gene family. **(a)** The number in the box represents the number of corresponding motifs contained in the 2 kb promoter sequence upstream of the gene. Blank indicates that the element is not included, and red and blue indicate the number of elements; the redder the color, the greater the number of elements with a given motif. **(b)** The various motifs are classified into four major categories: abiotic, hormone-related, development-related, and light-responsive, and each colored bar represents the number of element classifications contained in that gene. **(c–e)** The proportion of the number of each element in the three major categories of development-related, hormone-related, and abiotic, respectively.

**2.6. Expression Patterns of *OsiWD40s* Genes in Different Tissues**

To verify the function of *OsiWD40s* identified in indica (R498), expression profile data were obtained from the MBK database, the expression data of *OsiWD40s* in tissues and organs at different periods were analyzed, and a heat map was drawn based on their expression (Figure 6). There were three spatial-temporal expression patterns of *OsiWD40s*: the first category, *OsiWD40-8/12/44/48/51*, was expressed in panicle, spike and flower, with lower expression at root and leaf; the second category (e.g., *OsiWD40-4/27*), in contrast to the first category, had high expression at root and leaf and low expression in pollen; the third category (e.g., *OsiWD40-14/18*) was expressed in all tissues and organs at specific times, with constitutive expression. In addition, collinear gene pairs such as *OsiWD40-5/OsiWD40-38* had similar expression patterns, both expressed in roots, leaves, etc., and low expression in pollen, suggesting that some *OsiWD40s* genes are functionally redundant. In contrast, some collinear gene pairs, such as *OsiWD40-12/OsiWD40-29*, had opposite expression patterns, with the former being expressed in pollen and the latter in roots



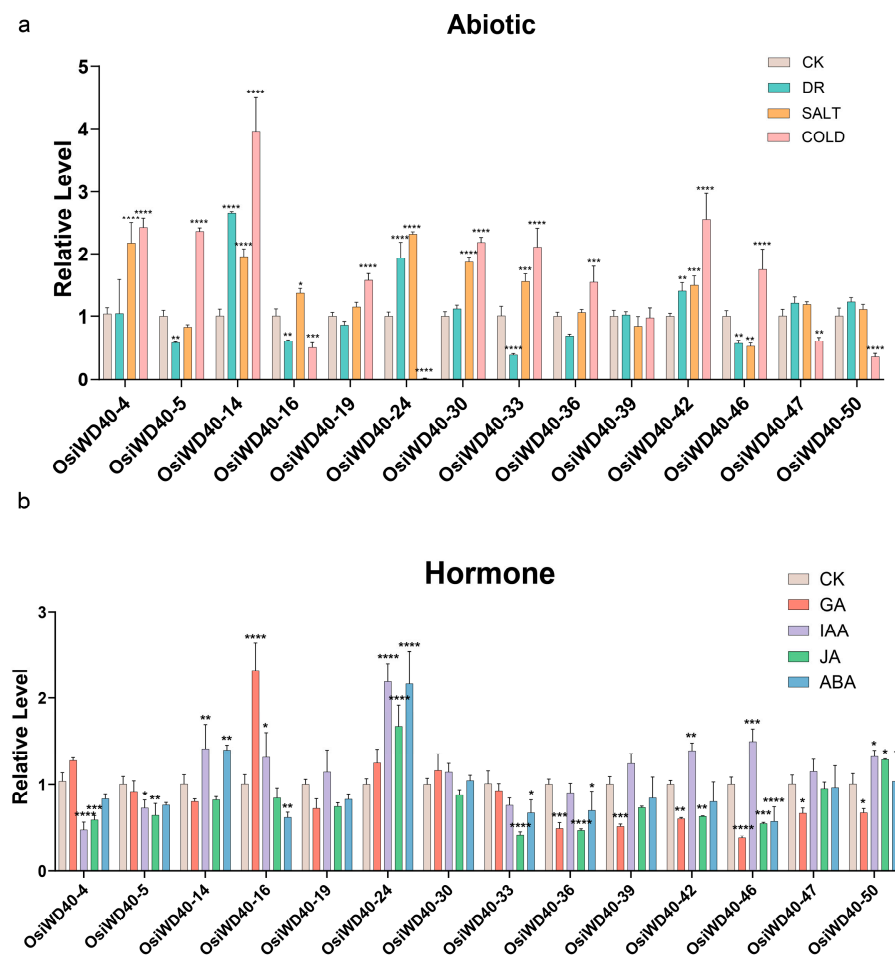


**Figure 7.** Relative expression level of 14 OsiWD40s in response to abiotic and hormone treatments. Error bars are standard deviations of three biological replicates. Asterisks were used to indicate the significant degree of the expression level compared to control. (\*  $p < 0.05$ , \*\*  $p < 0.01$ , \*\*\*  $p < 0.001$ , \*\*\*\*  $p < 0.0001$ ) (a) Abiotic treatments. CK: control, DR: drought, SALT: salt, COLD: cold. (b) Hormone treatments: CK: control, GA: gibberellic acid, IAA: auxin, JA: methyl Jasmonate, ABA: abscisic acid.

### 3. Discussion

The WD40 protein family is a large and diverse superfamily whose repeats, WD40, encode proteins containing a glycine-histidine (GH) pair at the N-terminal end and a tryptophan-aspartate (WD) pair at the C-terminal end, which play important roles in a wide range of physiological functions including growth, cell cycle, signal transduction, chromatin remodeling, and transcriptional regulation [44]. The WD40 repeat sequence is presumed to be caused by genomic duplication events and recombination [3,45].

In previous studies, 237, 200, 743, and 225 WD40 genes were identified in *Arabidopsis*, *japonica*, wheat, and *foxtail millet*, respectively [18,46,47]. In addition, 161 WD40 subfamily DWD proteins were identified in soybeans [48]. The presence of abundant WD40 genes in these plants indicates an evolutionary amplification of this superfamily. In addition to higher eukaryotes, such as rice, WD40 has been found in prokaryotes and lower organisms [12,49]. To date, the cloning and functional studies of WD40 genes in rice have been limited. It has been found that rice pollen germination regulator (GORI) encodes a WD40 protein essential for rice pollen growth [50,51], the SRWD1-WD40 subfamily of proteins regulated by salt stress [52], and that salt tolerance of rice seedlings can be enhanced by overexpression of the *OsABT* gene, which encodes a WD40 repeat protein [53].

WD40 protein family is involved in the anthocyanin synthesis pathway. Anthocyanin is favorable for the dietary management of metabolic disorders such as diabetes and

hyperlipidemia [54]. And anthocyanin in pigmented rice is beneficial to human health and can also be used as a natural pigment and nutraceutical [55,56]. Additionally, the purple coloration of the non-edible part was used in breeding programs as a morphological marker to identify the varieties and to study the linkage analysis [57]. At present, the anthocyanin synthesis-related WD40 gene in rice has only been cloned and studied by *OsTTG1* [30]. Studies have demonstrated that *OsTTG1* is localized in the nucleus and physically interacts with Kala4, *OsC1*, *OsDFR*, and Rc. There are 59 transcription factors that might be involved in influencing anthocyanin synthesis, and *OsWD40-3* (*LOC\_Os01g28680*) might be functionally redundant with *OsTTG1*. In this study, the WD40 subfamily in the *Oryza* genus was identified and analyzed for its characteristics, sequence structure, linkage, and cis-acting elements. In addition, the expression profiles of WD40 were analyzed by a combination of RNA-Seq and qRT-PCR to provide further insight into their functions.

Comparative genomics analysis in allied species can greatly improve the understanding of gene evolution. Based on the previous classification of the WD40 superfamily in japonica, the members of the subfamily in which WD40-TTG1 is located, the *Oryza* genus, were analyzed and validated. A total of 51 members were finally identified in *O. sativa*, 48 in *O. nivara*, 48 in *O. rufipogon*, 46 in *O. glaberrima*, 37 in *O. meridionalis*, 48 in *O. barthii*, 46 in *O. glumaepatula*, and 9 in *O. longistaminata*. The 383 members, including *O. sativa* and japonica, were divided into four groups based on the topology. The present study enriches the understanding of the WD40 family in eukaryotes, especially in the *Oryza* genus. Moreover, transposition, segmental duplication, and tandem duplication play an important role in biological evolution [58]. In this study, all gene pairs undergoing duplication events were generated by segmental duplication or WGD duplication, suggesting that segmental duplication or WGD duplication might have a large role in the *Oryza* genus, and they are mainly from subgroups B and C. Therefore, it can be inferred that segmental duplication is an important driver for the expansion of specific subfamilies of WD40s. The Ka/Ks ratio can determine whether the genes encoding proteins are subject to selection pressure [59]. The Ka/Ks analysis in this study showed that all duplicated WD40 gene pairs in the AA genome underwent purifying selection, suggesting that the elimination of unfavorable mutations might facilitate adaptation to complex environments in rice.

Genes with similar amino acid sequences will usually have similar functions [60]. In this study, *OsiWD40-15*, a member of the WD40 family in indica, showed the highest similarity to TTG1s of other plants with 61.42%, 99.70%, 58.77%, 61.31%, 61.18%, 61.88%, 61.47%, 59.76% identity to *AtTTG1*, *OsTTG1*, *BvTTG1*, *RsTTG1*, *MdTTG1*, *RrTTG1*, *PyTTG1*, and *PgTTG1*, respectively [61–65]. In addition, *OsiWD40-15* shares four highly conserved WDR motifs with other TTG1s, which might be related to anthocyanin biosynthesis. In most cases, the ternary complex MYB-bHLH-WD40 is an important player in the activation of structural genes for phycocyanin biosynthesis [27]. The protein–protein interactions analysis showed that *OsiWD40-15* might be interacting with MYB and bHLH transcription factors. It can be inferred that *OsiWD40-15* might also be able to participate in the anthocyanin synthesis pathway as a member of the MBW complex. In addition to analyzing the *Oryza* genus, interspecies evolutionary analyses of WD40 could be performed in more gramineous plants. However, some possible protein interactions were not validated in this study. Moreover, WD40 is usually carried out as one of the MBW complex components in the anthocyanin synthesis pathway. The MYB and bHLH transcription factors that might interact with WD40 can be studied in further studies, such as yeast two-hybrid hybridization and subcellular localization. Moreover, relevant candidate genes can be explored for breeding.

#### 4. Materials and Methods

##### 4.1. Plant Material, Growth, and Stress Conditions

Rice material 9311 (*Indica*, *Oryza sativa*) was cultured in a 26 °C chamber at Wuhan University, Wuhan, China with a light/dark photoperiod of 16/8 h and 60% relative humidity [66]. To study the response of *OsiWD40s* to hormone and abiotic stresses, plants

were subjected to different treatments at the three-leaf stage, such as 100  $\mu$ M Abscisic acid (ABA), 50  $\mu$ M 3-Indole acetic acid (IAA), 50  $\mu$ M Gibberellic acid (GA), 100  $\mu$ M Methyl Jasmonate (MeJA), 120 mM NaCl (salt treatment), 25% polyethylene glycol (PEG 6000, drought treatment), and 5 low temperatures (cold treatment). The reagents used were obtained from Biosharp, Anhui, China, and MACKLIN, Wuhan, China. The solution with the configured concentration was added to the liquid medium respectively, and leaves were collected after 24 h treatments and stored at  $-80$  °C. Three biological replicates were used for each treatment.

#### 4.2. Identification and Phylogenetic Analysis of WD40 Genes in Rice

The whole genome datasets of *O. nivara*, *O. rufipogon*, *O. glaberrima*, *O. meridionalis*, *O. barthii*, *O. glumaepatula* and *O. longistaminata* from Ensemble Plant "<http://plants.ensembl.org/index.html> (accessed on 25 October 2022)", data of *O. sativa indica*(R498) from MBKbase "<https://mbkbase.org/rice> (accessed on 25 October 2022)", and data of *O. sativa japonica* (*Nipponbare*) from Rice Genome Annotation Project "<http://rice.uga.edu/> (accessed on 25 October 2022)". Next, the HMM (Hidden Markov Model) file of WD40 (PF00400) was obtained from the Pfam database "<http://pfam-legacy.xfam.org/> (accessed on 25 October 2022)" and used as query to search for eight species using HMMER v3.3.2 [67,68]. Then, 50 *OsWD40s* protein sequences extracted from *O. sativa japonica* were used as query sequences to search the local protein database (E-value of  $e^{-5}$ ) by BLASTP software (v2.14.1). Then, the results of HMMER and BLASTP methods were intersected [69]. Then, all candidate WD40 protein sequences were tested for the presence of the WD40 structural domain using the hmmscan program of HMMER. All WD40 gene accession names are shown in Table S1. The identified WD40 protein sequences were subjected to multiple sequence alignment using mafft v7.475 default parameters [70]. Subsequently, phylogenetic trees were constructed using fasttree based on the maximum likelihood method with default parameters [71]. The species tree was obtained from TimeTree "<http://www.timetree.org/> (accessed on 29 August 2023)" based on the divergence time [72]. Finally, they were uploaded to iTOL online tool "<https://itol.embl.de/> (accessed on 14 June 2023)" for further refinement [73].

#### 4.3. Chromosomal Localization, Gene Structure, and Conserved Motifs

To obtain the genomic distribution of the WD40s, chromosomal location and gene structure information of the members were extracted from the GFF3 file and further visualized by TBtools. Then, TBtools was used to provide a comprehensive analysis of the physical and chemical properties of *WD40s*, and amino acid size, isoelectric point, and molecular weight were analyzed with TBtools [74]. In addition, the WD40s protein sequence was uploaded to BUSCA "<http://busca.biocomp.unibo.it/> (accessed on 30 August 2023)" for protein subcellular localization prediction [75]. Then, MEME 5.5.0 (parameters: -protein -oc -nostatus -time 14,400 -mod zoops -nmotifs 10 -minw 6 -maxw 50 -objfun classic -markov\_order 0) to identify up to 10 conserved motifs in these proteins [76]. The motif information is shown in Table S4. Then, motifs were uploaded to Tomtom "[https://meme-suite.org/meme/doc/tomtom.html?man\\_type=web](https://meme-suite.org/meme/doc/tomtom.html?man_type=web) (accessed on 12 October 2023)" and analyzed the sequences in which the motifs might code [77]. Subsequently, a 2000 bp sequence upstream of the WD40 gene was extracted using TBtools, and cis-acting elements were retrieved through the PlantCARE online tool "<http://bioinformatics.psb.ugent.be/webtools/plantcare/html/> (accessed on 15 June 2023)".

#### 4.4. Collinearity Analysis of WD40 Genes

Collinearity analysis using the MCScanX toolkit with default parameters to explore *WD40s* duplexing events in AA genome and visualization of collinear gene pairs using TBtools [78].  $K_a$ ,  $K_s$ , and  $K_a/K_s$  ratios of duplicated genes were calculated using TBtools' simple  $K_a/K_s$  calculator. Divergence time (T) was calculated as  $T = K_s / (2 \times 6.5 \times 10^{-9}) \times 10^{-6}$  million years ago (Mya) [79].

#### 4.5. Expression and Interaction Analysis of *OsiWD40* Gene Family

Expression profile data of *OsiWD40s* at different stages in multiple tissues were retrieved from the MBKbase database “<https://mbkbase.org/rice> (accessed on 21 June 2023)” [80], and pheatmap package of R software (4.1.2) was used to plot heatmap. STRING database “<https://cn.string-db.org> (accessed on 28 June 2023)” was used to predict the protein-interaction relationship of *OsiWD40* [81].

#### 4.6. RNA Extraction and qPCR Analysis

Total RNA of the samples was extracted using FastPure Plant Total RNA Isolation Kit. First-strand cDNA was synthesized using UEIris RT mix with DNase (all-in-one), and Hieff UNICON Universal Blue qPCR SYBR Green Master Mix was used for quantitative analysis according to the instructions. Untreated samples were used as controls, and three technical replicates were performed for each gene. qRT-PCR reactions were performed on a CFX96 Touch™ Real-Time PCR Detection System (Bio-Rad, Hercules, CA, USA) with the following thermal cycling conditions: pre-denaturation at 95 °C for 10 min, denaturation at 95 °C for 10 s, annealing at 60 °C for 10 s, and 72 °C extension for 15 s. The reactions were repeated for 40 cycles, and solubility curves were plotted from 65 °C to 95 °C to test the specificity of the primers. The actin gene (*UBI*) was used as an internal reference control, and the primers used are shown in Table S3. Relative expression levels were calculated based on three biological replicates using the  $2^{-\Delta\Delta CT}$  method [82]. A two-way ANOVA was performed on the data, and the results were visualized in GraphPad Prism9.

### 5. Conclusions

In this study, 383 WD40 subfamily members were identified in the *Oryza* genus and classified into four groups. These first analyzed the evolutionary patterns of the WD40 subfamily in multiple species. They have similar chromosome distribution and physiological characteristics. In addition, segmental duplication was the main expansion pattern during the WD40 gene family evolution, and collinearity was similar in the *Oryza* genus. As an example, the expression analysis in indica showed that WD40 genes might be involved in the growth and development of several tissues and organs, such as roots, stems, leaves, and flowers. Many metabolic elements, hormone response elements, and stress response elements were found in the promoter region. In addition, the expression patterns in indica were analyzed under various phytohormonal and abiotic stresses, and some genes played important roles in the growth and stress tolerance process. These results provide new insights into the functions of the WD40 family in species evolution and rice development and have potential applications in breeding for rice quality improvement.

**Supplementary Materials:** The following supporting information can be downloaded at: <https://www.mdpi.com/article/10.3390/ijms242115776/s1>.

**Author Contributions:** Conceptualization, S.K. and Y.L.; data curation, S.K., Y.J. and M.Z.; writing—original draft preparation, S.K.; writing—review and editing, S.K. and Y.L.; visualization, S.K.; supervision, Y.L. All authors have read and agreed to the published version of the manuscript.

**Funding:** This study was funded by the National Key Research and Development Program of China. (Grant No. 2016YFD0100400) and the National Special Key Project for Transgenic Breeding (Grant No. 2016ZX08001001).

**Institutional Review Board Statement:** Not applicable.

**Informed Consent Statement:** Not applicable.

**Data Availability Statement:** Data are contained within the article or Supplementary Material.

**Conflicts of Interest:** The authors declare no conflict of interest.

## References

1. Stirnimann, C.U.; Petsalaki, E.; Russell, R.B.; Müller, C.W. WD40 Proteins Propel Cellular Networks. *Trends Biochem. Sci.* **2010**, *35*, 565–574. [[CrossRef](#)]
2. Fong, H.K.; Hurley, J.B.; Hopkins, R.S.; Miake-Lye, R.; Johnson, M.S.; Doolittle, R.F.; Simon, M.I. Repetitive Segmental Structure of the Transducin Beta Subunit: Homology with the CDC4 Gene and Identification of Related mRNAs. *Proc. Natl. Acad. Sci. USA* **1986**, *83*, 2162–2166. [[CrossRef](#)]
3. Andrade, M.A.; Perez-Iratxeta, C.; Ponting, C.P. Protein Repeats: Structures, Functions, and Evolution. *J. Struct. Biol.* **2001**, *134*, 117–131. [[CrossRef](#)]
4. Schapira, M.; Tyers, M.; Torrent, M.; Arrowsmith, C.H. WD40 Repeat Domain Proteins: A Novel Target Class? *Nat. Rev. Drug Discov.* **2017**, *16*, 773–786. [[CrossRef](#)]
5. Smith, T.F. Diversity of WD-Repeat Proteins. *Subcell. Biochem.* **2008**, *48*, 20–30. [[CrossRef](#)] [[PubMed](#)]
6. Jennings, B.H.; Pickles, L.M.; Wainwright, S.M.; Roe, S.M.; Pearl, L.H.; Ish-Horowicz, D. Molecular Recognition of Transcriptional Repressor Motifs by the WD Domain of the Groucho/TLE Corepressor. *Mol. Cell* **2006**, *22*, 645–655. [[CrossRef](#)]
7. Jain, B.P.; Pandey, S. WD40 Repeat Proteins: Signalling Scaffold with Diverse Functions. *Protein J.* **2018**, *37*, 391–406. [[CrossRef](#)]
8. Guerriero, G.; Hausman, J.-F.; Ezcurra, I. WD40-Repeat Proteins in Plant Cell Wall Formation: Current Evidence and Research Prospects. *Front. Plant Sci.* **2015**, *6*, 1112. [[CrossRef](#)] [[PubMed](#)]
9. Zhang, C.; Zhang, F. The Multifunctions of WD40 Proteins in Genome Integrity and Cell Cycle Progression. *J. Genom.* **2015**, *3*, 40–50. [[CrossRef](#)] [[PubMed](#)]
10. Gurung, R.; Om, D.; Pun, R.; Hyun, S.; Shin, D. Recent Progress in Modulation of WD40-Repeat Domain 5 Protein (WDR5): Inhibitors and Degraders. *Cancers* **2023**, *15*, 3910. [[CrossRef](#)]
11. Hu, X.-J.; Li, T.; Wang, Y.; Xiong, Y.; Wu, X.-H.; Zhang, D.-L.; Ye, Z.-Q.; Wu, Y.-D. Prokaryotic and Highly-Repetitive WD40 Proteins: A Systematic Study. *Sci. Rep.* **2017**, *7*, 10585. [[CrossRef](#)]
12. Guo, M.; Wang, J.; Zhang, Y.; Zhang, L. Increased WD40 Motifs in *Planctomycete bacteria* and Their Evolutionary Relevance. *Mol. Phylogenet. Evol.* **2021**, *155*, 107018. [[CrossRef](#)] [[PubMed](#)]
13. Rai, K.K.; Singh, S.; Rai, R.; Rai, L.C. Functional Characterization of Two WD40 Family Proteins, Alr0671 and All2352, from *Anabaena PCC 7120* and Deciphering Their Role in Abiotic Stress Management. *Plant Mol. Biol.* **2022**, *110*, 545–563. [[CrossRef](#)] [[PubMed](#)]
14. Tan, L.; Salih, H.; Htet, N.N.W.; Azeem, F.; Zhan, R. Genomic Analysis of WD40 Protein Family in the Mango Reveals a TTG1 Protein Enhances Root Growth and Abiotic Tolerance in Arabidopsis. *Sci. Rep.* **2021**, *11*, 2266. [[CrossRef](#)]
15. Van Nocker, S.; Ludwig, P. The WD-Repeat Protein Superfamily in Arabidopsis: Conservation and Divergence in Structure and Function. *BMC Genom.* **2003**, *4*, 50. [[CrossRef](#)] [[PubMed](#)]
16. Feng, R.; Zhang, C.; Ma, R.; Cai, Z.; Lin, Y.; Yu, M. Identification and Characterization of WD40 Superfamily Genes in Peach. *Gene* **2019**, *710*, 291–306. [[CrossRef](#)]
17. Chen, S.; Li, D.; Chen, S.; He, J.; Wang, Z.; Yang, G.; Lu, Z. Identifying and Expression Analysis of WD40 Transcription Factors in Walnut. *Plant Genome* **2022**, *15*, e20229. [[CrossRef](#)]
18. Ouyang, Y.; Huang, X.; Lu, Z.; Yao, J. Genomic Survey, Expression Profile and Co-Expression Network Analysis of OsWD40 Family in Rice. *BMC Genom.* **2012**, *13*, 100. [[CrossRef](#)]
19. Wang, Y.; Hu, X.-J.; Zou, X.-D.; Wu, X.-H.; Ye, Z.-Q.; Wu, Y.-D. WDSPdb: A Database for WD40-Repeat Proteins. *Nucleic Acids Res.* **2015**, *43*, D339–D344. [[CrossRef](#)]
20. Dayebgadoh, G.; Sardi, M.E.; Florens, L.; Washburn, M.P. Biochemical Reduction of the Topology of the Diverse WDR76 Protein Interactome. *J. Proteome Res.* **2019**, *18*, 3479–3491. [[CrossRef](#)]
21. Park, H.J.; Baek, D.; Cha, J.-Y.; Liao, X.; Kang, S.-H.; McClung, C.R.; Lee, S.Y.; Yun, D.-J.; Kim, W.-Y. HOS15 Interacts with the Histone Deacetylase HDA9 and the Evening Complex to Epigenetically Regulate the Floral Activator GIGANTEA. *Plant Cell* **2019**, *31*, 37–51. [[CrossRef](#)]
22. Xu, X.; Wan, W.; Jiang, G.; Xi, Y.; Huang, H.; Cai, J.; Chang, Y.; Duan, C.-G.; Mangrauthia, S.K.; Peng, X.; et al. Nucleocytoplasmic Trafficking of the Arabidopsis WD40 Repeat Protein XIW1 Regulates ABI5 Stability and Abscisic Acid Responses. *Mol. Plant* **2019**, *12*, 1598–1611. [[CrossRef](#)] [[PubMed](#)]
23. Kwantes, M.; Wichard, T. The APAF1\_C/WD40 Repeat Domain-Encoding Gene from the Sea Lettuce *Ulva Mutabilis* Sheds Light on the Evolution of NB-ARC Domain-Containing Proteins in Green Plants. *Planta* **2022**, *255*, 76. [[CrossRef](#)] [[PubMed](#)]
24. Kong, D.; Li, M.; Dong, Z.; Ji, H.; Li, X. Identification of TaWD40D, a Wheat WD40 Repeat-Containing Protein That Is Associated with Plant Tolerance to Abiotic Stresses. *Plant Cell Rep.* **2015**, *34*, 395–410. [[CrossRef](#)]
25. Zhu, F.; Jadhav, S.S.; Tohge, T.; Salem, M.A.; Lee, J.M.; Giovannoni, J.J.; Cheng, Y.; Alseikh, S.; Fernie, A.R. A Comparative Transcriptomics and eQTL Approach Identifies SIWD40 as a Tomato Fruit Ripening Regulator. *Plant Physiol.* **2022**, *190*, 250–266. [[CrossRef](#)] [[PubMed](#)]
26. Gao, X.; Chen, Z.; Zhang, J.; Li, X.; Chen, G.; Li, X.; Wu, C. OsLIS-L1 Encoding a Lissencephaly Type-1-like Protein with WD40 Repeats Is Required for Plant Height and Male Gametophyte Formation in Rice. *Planta* **2012**, *235*, 713–727. [[CrossRef](#)]
27. Mackon, E.; Jeazet Dongho Epse Mackon, G.C.; Ma, Y.; Haneef Kashif, M.; Ali, N.; Usman, B.; Liu, P. Recent Insights into Anthocyanin Pigmentation, Synthesis, Trafficking, and Regulatory Mechanisms in Rice (*Oryza sativa* L.) Caryopsis. *Biomolecules* **2021**, *11*, 394. [[CrossRef](#)]

28. Baudry, A.; Heim, M.A.; Dubreucq, B.; Caboche, M.; Weisshaar, B.; Lepiniec, L. TT2, TT8, and TTG1 Synergistically Specify the Expression of *BANYULS* and Proanthocyanidin Biosynthesis in *Arabidopsis thaliana*. *Plant J.* **2004**, *39*, 366–380. [[CrossRef](#)]
29. Zhang, B.; Schrader, A. TRANSPARENT TESTA GLABRA 1-Dependent Regulation of Flavonoid Biosynthesis. *Plants* **2017**, *6*, 65. [[CrossRef](#)]
30. Yang, X.; Wang, J.; Xia, X.; Zhang, Z.; He, J.; Nong, B.; Luo, T.; Feng, R.; Wu, Y.; Pan, Y.; et al. *OsTTG1*, a WD40 Repeat Gene, Regulates Anthocyanin Biosynthesis in Rice. *Plant J.* **2021**, *107*, 198–214. [[CrossRef](#)]
31. Liu, Y.; Hou, H.; Jiang, X.; Wang, P.; Dai, X.; Chen, W.; Gao, L.; Xia, T. A WD40 Repeat Protein from *Camellia sinensis* Regulates Anthocyanin and Proanthocyanidin Accumulation through the Formation of MYB–BHLH–WD40 Ternary Complexes. *Int. J. Mol. Sci.* **2018**, *19*, 1686. [[CrossRef](#)] [[PubMed](#)]
32. Jiu, S.; Guan, L.; Leng, X.; Zhang, K.; Haider, M.S.; Yu, X.; Zhu, X.; Zheng, T.; Ge, M.; Wang, C.; et al. The Role of VvMYBA2r and VvMYBA2w Alleles of the MYBA2 Locus in the Regulation of Anthocyanin Biosynthesis for Molecular Breeding of Grape (*Vitis* Spp.) Skin Coloration. *Plant Biotechnol. J.* **2021**, *19*, 1216–1239. [[CrossRef](#)] [[PubMed](#)]
33. Allen, P.J.; Napoli, R.S.; Parish, R.W.; Li, S.F. MYB-bHLH-TTG1 in a Multi-Tiered Pathway Regulates Arabidopsis Seed Coat Mucilage Biosynthesis Genes Including PECTIN METHYLESTERASE INHIBITOR14 Required for Homogalacturonan Demethylesterification. *Plant Cell Physiol.* **2023**, *64*, pcd065. [[CrossRef](#)] [[PubMed](#)]
34. Long, Y.; Schiefelbein, J. Novel TTG1 Mutants Modify Root-Hair Pattern Formation in Arabidopsis. *Front. Plant Sci.* **2020**, *11*, 383. [[CrossRef](#)]
35. Yu, C.-Y.; Sharma, O.; Nguyen, P.H.T.; Hartono, C.D.; Kanehara, K. A Pair of DUF538 Domain-Containing Proteins Modulates Plant Growth and Trichome Development through the Transcriptional Regulation of GLABRA1 in *Arabidopsis thaliana*. *Plant J.* **2021**, *108*, 992–1004. [[CrossRef](#)]
36. Paffendorf, B.A.M.; Qassrawi, R.; Meys, A.M.; Trimborn, L.; Schrader, A. TRANSPARENT TESTA GLABRA 1 Participates in Flowering Time Regulation in Arabidopsis Thaliana. *PeerJ* **2020**, *8*, e8303. [[CrossRef](#)]
37. Guo, Y.; Zhao, H.; Wang, Y.; Zhang, T.; Wang, Z.; Chen, X.; Zhang, X.; Li, Z.; Shen, J. TARGET OF EAT3 (TOE3) Specifically Regulates Fruit Spine Initiation in Cucumber (*Cucumis sativus* L.). *Plant J.* **2023**, *115*, 678–689. [[CrossRef](#)]
38. Huang, X.; Yi, P.; Liu, Y.; Li, Q.; Jiang, Y.; Yi, Y.; Yan, H. RrTTG1 Promotes Fruit Prickle Development through an MBW Complex in *Rosa roxburghii*. *Front. Plant Sci.* **2022**, *13*, 939270. [[CrossRef](#)]
39. Tian, H.; Wang, S. TRANSPARENT TESTA GLABRA1, a Key Regulator in Plants with Multiple Roles and Multiple Function Mechanisms. *Int. J. Mol. Sci.* **2020**, *21*, 4881. [[CrossRef](#)]
40. Qiu, Y.; Tao, R.; Feng, Y.; Xiao, Z.; Zhang, D.; Peng, Y.; Wen, X.; Wang, Y.; Guo, H. EIN3 and RSL4 Interfere with an MYB–bHLH–WD40 Complex to Mediate Ethylene-Induced Ectopic Root Hair Formation in Arabidopsis. *Proc. Natl. Acad. Sci. USA* **2021**, *118*, e2110004118. [[CrossRef](#)]
41. Broucke, E.; Dang, T.T.V.; Li, Y.; Hulsmans, S.; Van Leene, J.; De Jaeger, G.; Hwang, I.; Wim, V.d.E.; Rolland, F. SnRK1 Inhibits Anthocyanin Biosynthesis through Both Transcriptional Regulation and Direct Phosphorylation and Dissociation of the MYB/bHLH/TTG1 MBW Complex. *Plant J.* **2023**, *115*, 1193–1213. [[CrossRef](#)] [[PubMed](#)]
42. Yamagata, Y.; Win, K.T.; Miyazaki, Y.; Ogata, C.; Yasui, H.; Yoshimura, A. Development of Introgression Lines of AA Genome *Oryza* Species, *O. glaberrima*, *O. rufipogon*, and *O. nivara*, in the Genetic Background of *O. sativa* L. cv. Taichung 65. *Breed. Sci.* **2019**, *69*, 359–363. [[CrossRef](#)]
43. Zhang, Y.; Zhou, J.; Xu, P.; Li, J.; Deng, X.; Deng, W.; Yang, Y.; Yu, Y.; Pu, Q.; Tao, D. A Genetic Resource for Rice Improvement: Introgression Library of Agronomic Traits for All AA Genome *Oryza* Species. *Front. Plant Sci.* **2022**, *13*, 856514. [[CrossRef](#)] [[PubMed](#)]
44. Smith, T.F.; Gaitatzes, C.; Saxena, K.; Neer, E.J. The WD Repeat: A Common Architecture for Diverse Functions. *Trends Biochem. Sci.* **1999**, *24*, 181–185. [[CrossRef](#)]
45. Makarova, K.S.; Wolf, Y.I.; Mekhedov, S.L.; Mirkin, B.G.; Koonin, E.V. Ancestral Paralogs and Pseudoparalogs and Their Role in the Emergence of the Eukaryotic Cell. *Nucleic Acids Res.* **2005**, *33*, 4626–4638. [[CrossRef](#)]
46. Mishra, A.K.; Muthamilarasan, M.; Khan, Y.; Parida, S.K.; Prasad, M. Genome-Wide Investigation and Expression Analyses of WD40 Protein Family in the Model Plant Foxtail Millet (*Setaria italica* L.). *PLoS ONE* **2014**, *9*, e86852. [[CrossRef](#)]
47. Hu, R. Genome-Wide Identification and Analysis of WD40 Proteins in Wheat (*Triticum aestivum* L.). *BMC Genom.* **2018**, *19*, 303.
48. Bian, S.; Li, X.; Mainali, H.; Chen, L.; Dhaubhadel, S. Genome-Wide Analysis of DWD Proteins in Soybean (*Glycine max*): Significance of Gm08DWD and GmMYB176 Interaction in Isoflavonoid Biosynthesis. *PLoS ONE* **2017**, *12*, e0178947. [[CrossRef](#)] [[PubMed](#)]
49. Roling, L.; Flammersfeld, A.; Pradel, G.; Bennink, S. The WD40-Protein PfWLP1 Ensures Stability of the PfCCp-Based Adhesion Protein Complex in Plasmodium Falciparum Gametocytes. *Front. Cell. Infect. Microbiol.* **2022**, *12*, 942364. [[CrossRef](#)]
50. Kim, Y.; Kim, M.; Hong, W.; Moon, S.; Kim, E.; Silva, J.; Lee, J.; Lee, S.; Kim, S.T.; Park, S.K.; et al. GORI, Encoding the WD40 Domain Protein, Is Required for Pollen Tube Germination and Elongation in Rice. *Plant J.* **2021**, *105*, 1645–1664. [[CrossRef](#)]
51. Kim, Y.-J.; Jung, K.-H. WD40-Domain Protein GORI Is an Integrative Scaffold That Is Required for Pollen Tube Growth in Rice. *Plant Signal. Behav.* **2023**, *18*, 2082678. [[CrossRef](#)] [[PubMed](#)]
52. Huang, J.; Wang, M.-M.; Bao, Y.-M.; Sun, S.-J.; Pan, L.-J.; Zhang, H.-S. SRWD: A Novel WD40 Protein Subfamily Regulated by Salt Stress in Rice (*Oryza sativa* L.). *Gene* **2008**, *424*, 71–79. [[CrossRef](#)] [[PubMed](#)]

53. Wen, D.; Bao, L.; Huang, X.; Qian, X.; Chen, E.; Shen, B. OsABT Is Involved in Abscisic Acid Signaling Pathway and Salt Tolerance of Roots at the Rice Seedling Stage. *Int. J. Mol. Sci.* **2022**, *23*, 10656. [[CrossRef](#)] [[PubMed](#)]
54. Aalim, H.; Wang, D.; Luo, Z. Black Rice (*Oryza sativa* L.) Processing: Evaluation of Physicochemical Properties, In Vitro Starch Digestibility, and Phenolic Functions Linked to Type 2 Diabetes. *Food Res. Int.* **2021**, *141*, 109898. [[CrossRef](#)]
55. Leonarski, E.; Kuasnei, M.; Cesca, K.; Oliveira, D.D.; Zielinski, A.A.F. Black Rice and Its By-Products: Anthocyanin-Rich Extracts and Their Biological Potential. *Crit. Rev. Food Sci. Nutr.* **2023**, 1–19. [[CrossRef](#)]
56. Yi, J.; Qiu, M.; Zhu, Z.; Dong, X.; Andrew Decker, E.; McClements, D.J. Robust and Recyclable Magnetic Nanobiocatalysts for Extraction of Anthocyanin from Black Rice. *Food Chem.* **2021**, *364*, 130447. [[CrossRef](#)]
57. Tsago, Y.; Wang, Z.; Liu, J.; Sunusi, M.; Eshag, J.; Akhter, D.; Shi, C.; Jin, X. Morphological Characteristics and Gene Mapping of Purple Apiculus Formation in Rice. *Plant Mol. Biol. Rep.* **2019**, *37*, 277–290. [[CrossRef](#)]
58. Xu, G.; Guo, C.; Shan, H.; Kong, H. Divergence of Duplicate Genes in Exon-Intron Structure. *Proc. Natl. Acad. Sci. USA* **2012**, *109*, 1187–1192. [[CrossRef](#)]
59. Hurst, L.D. The Ka/Ks Ratio: Diagnosing the Form of Sequence Evolution. *Trends Genet.* **2002**, *18*, 486. [[CrossRef](#)]
60. Liu, J.; Zhang, C.; Han, J.; Fang, X.; Xu, H.; Liang, C.; Li, D.; Yang, Y.; Cui, Z.; Wang, R.; et al. Genome-Wide Analysis of KNOX Transcription Factors and Expression Pattern of Dwarf-Related KNOX Genes in Pear. *Front. Plant Sci.* **2022**, *13*, 806765. [[CrossRef](#)]
61. Tabata, S.; Kaneko, T.; Nakamura, Y.; Kotani, H.; Kato, T.; Asamizu, E.; Miyajima, N.; Sasamoto, S.; Kimura, T.; Hosouchi, T.; et al. Sequence and Analysis of Chromosome 5 of the Plant *Arabidopsis thaliana*. *Nature* **2000**, *408*, 823–826. [[CrossRef](#)]
62. Lim, S.-H.; Kim, D.-H.; Lee, J.-Y. RsTTG1, a WD40 Protein, Interacts with the bHLH Transcription Factor RsTT8 to Regulate Anthocyanin and Proanthocyanidin Biosynthesis in *Raphanus sativus*. *Int. J. Mol. Sci.* **2022**, *23*, 11973. [[CrossRef](#)] [[PubMed](#)]
63. Brueggemann, J.; Weisshaar, B.; Sagasser, M. A WD40-Repeat Gene from *Malus x domestica* Is a Functional Homologue of *Arabidopsis thaliana* TRANSPARENT TESTA GLABRA1. *Plant Cell Rep.* **2010**, *29*, 285–294. [[CrossRef](#)] [[PubMed](#)]
64. Cui, D.; Zhao, S.; Xu, H.; Allan, A.C.; Zhang, X.; Fan, L.; Chen, L.; Su, J.; Shu, Q.; Li, K. The Interaction of MYB, bHLH and WD40 Transcription Factors in Red Pear (*Pyrus pyrifolia*) Peel. *Plant Mol. Biol.* **2021**, *106*, 407–417. [[CrossRef](#)] [[PubMed](#)]
65. Ben-Simhon, Z.; Judeinstein, S.; Nadler-Hassar, T.; Trainin, T.; Bar-Ya'akov, I.; Borochoy-Neori, H.; Holland, D. A Pomegranate (*Punica granatum* L.) WD40-Repeat Gene Is a Functional Homologue of *Arabidopsis* TTG1 and Is Involved in the Regulation of Anthocyanin Biosynthesis during Pomegranate Fruit Development. *Planta* **2011**, *234*, 865–881. [[CrossRef](#)]
66. Kong, W.; Zhang, Y.; Deng, X.; Li, S.; Zhang, C.; Li, Y. Comparative Genomic and Transcriptomic Analysis Suggests the Evolutionary Dynamic of GH3 Genes in Gramineae Crops. *Front. Plant Sci.* **2019**, *10*, 1297. [[CrossRef](#)]
67. Potter, S.C.; Luciani, A.; Eddy, S.R.; Park, Y.; Lopez, R.; Finn, R.D. HMMER Web Server: 2018 Update. *Nucleic Acids Res.* **2018**, *46*, W200–W204. [[CrossRef](#)]
68. Mistry, J.; Chuguransky, S.; Williams, L.; Qureshi, M.; Salazar, G.A.; Sonnhammer, E.L.L.; Tosatto, S.C.E.; Paladin, L.; Raj, S.; Richardson, L.J.; et al. Pfam: The Protein Families Database in 2021. *Nucleic Acids Res.* **2021**, *49*, D412–D419. [[CrossRef](#)]
69. Kong, W.; Sun, T.; Zhang, C.; Qiang, Y.; Li, Y. Micro-Evolution Analysis Reveals Diverged Patterns of Polyol Transporters in Seven Gramineae Crops. *Front. Genet.* **2020**, *11*, 565. [[CrossRef](#)]
70. Katoh, K.; Standley, D.M. MAFFT Multiple Sequence Alignment Software Version 7: Improvements in Performance and Usability. *Mol. Biol. Evol.* **2013**, *30*, 772–780. [[CrossRef](#)]
71. Price, M.N.; Dehal, P.S.; Arkin, A.P. FastTree: Computing Large Minimum Evolution Trees with Profiles Instead of a Distance Matrix. *Mol. Biol. Evol.* **2009**, *26*, 1641–1650. [[CrossRef](#)] [[PubMed](#)]
72. Kumar, S.; Suleski, M.; Craig, J.M.; Kasprowitz, A.E.; Sanderford, M.; Li, M.; Stecher, G.; Hedges, S.B. TimeTree 5: An Expanded Resource for Species Divergence Times. *Mol. Biol. Evol.* **2022**, *39*, msac174. [[CrossRef](#)] [[PubMed](#)]
73. Letunic, I.; Bork, P. Interactive Tree Of Life (iTOL) v5: An Online Tool for Phylogenetic Tree Display and Annotation. *Nucleic Acids Res.* **2021**, *49*, W293–W296. [[CrossRef](#)] [[PubMed](#)]
74. Chen, C.; Chen, H.; Zhang, Y.; Thomas, H.R.; Frank, M.H.; He, Y.; Xia, R. TBtools: An Integrative Toolkit Developed for Interactive Analyses of Big Biological Data. *Mol. Plant* **2020**, *13*, 1194–1202. [[CrossRef](#)]
75. Savojardo, C.; Martelli, P.L.; Fariselli, P.; Profiti, G.; Casadio, R. BUSCA: An Integrative Web Server to Predict Subcellular Localization of Proteins. *Nucleic Acids Res.* **2018**, *46*, W459–W466. [[CrossRef](#)]
76. Bailey, T.L.; Boden, M.; Buske, F.A.; Frith, M.; Grant, C.E.; Clementi, L.; Ren, J.; Li, W.W.; Noble, W.S. MEME SUITE: Tools for Motif Discovery and Searching. *Nucleic Acids Res.* **2009**, *37*, W202–W208. [[CrossRef](#)]
77. Gupta, S.; Stamatoyannopoulos, J.A.; Bailey, T.L.; Noble, W.S. Quantifying Similarity between Motifs. *Genome Biol.* **2007**, *8*, R24. [[CrossRef](#)]
78. Wang, Y.; Tang, H.; Debarry, J.D.; Tan, X.; Li, J.; Wang, X.; Lee, T.; Jin, H.; Marler, B.; Guo, H.; et al. MCScanX: A Toolkit for Detection and Evolutionary Analysis of Gene Synteny and Collinearity. *Nucleic Acids Res.* **2012**, *40*, e49. [[CrossRef](#)]
79. Gaut, B.S.; Morton, B.R.; McCaig, B.C.; Clegg, M.T. Substitution Rate Comparisons between Grasses and Palms: Synonymous Rate Differences at the Nuclear Gene *Adh* Parallel Rate Differences at the Plastid Gene *rbcl*. *Proc. Natl. Acad. Sci. USA* **1996**, *93*, 10274–10279. [[CrossRef](#)]
80. Peng, H.; Wang, K.; Chen, Z.; Cao, Y.; Gao, Q.; Li, Y.; Li, X.; Lu, H.; Du, H.; Lu, M.; et al. MBKbase for Rice: An Integrated Omics Knowledgebase for Molecular Breeding in Rice. *Nucleic Acids Res.* **2020**, *48*, D1085–D1092. [[CrossRef](#)]

81. Szklarczyk, D.; Gable, A.L.; Nastou, K.C.; Lyon, D.; Kirsch, R.; Pyysalo, S.; Doncheva, N.T.; Legeay, M.; Fang, T.; Bork, P.; et al. The STRING Database in 2021: Customizable Protein-Protein Networks, and Functional Characterization of User-Uploaded Gene/Measurement Sets. *Nucleic Acids Res.* **2021**, *49*, D605–D612. [[CrossRef](#)] [[PubMed](#)]
82. Livak, K.J.; Schmittgen, T.D. Analysis of Relative Gene Expression Data Using Real-Time Quantitative PCR and the 2(-Delta Delta C(T)) Method. *Methods* **2001**, *25*, 402–408. [[CrossRef](#)] [[PubMed](#)]

**Disclaimer/Publisher’s Note:** The statements, opinions and data contained in all publications are solely those of the individual author(s) and contributor(s) and not of MDPI and/or the editor(s). MDPI and/or the editor(s) disclaim responsibility for any injury to people or property resulting from any ideas, methods, instructions or products referred to in the content.